# Step-height-tripling transition on vicinal Si(111)

R. J. Phaneuf and Ellen D. Williams
*Department of Physics and Astronomy, University of Maryland, College Park, Maryland 20742-4111*
(Received 5 June 1989)

We have used low-energy electron diffraction to characterize the temperature dependence of the structure of vicinal Si(111) surfaces misoriented by 6° and 12° toward the $[2\bar{1}\,\bar{1}]$ azimuthal direction. At high temperatures these surfaces contain a uniform density of steps of height close to the (111) double-layer spacing. As the temperature is lowered the step structure changes abruptly, and reversibly, at approximately 860 °C for both angles of misorientation. The changes in step structure occur simultaneously with the appearance of diffracted beams characteristic of the (7×7) reconstruction of the Si(111) surface. The step structure at low temperatures has triple the period of that of the high-temperature surface. The diffraction features, however, are inconsistent with a simple array of steps of height equal to three times the double-layer spacing, as we show by considering a simple diffraction model. The effect of the reconstructive transition on these $[2\bar{1}\,\bar{1}]$-misoriented Si(111) surfaces is contrasted with previous observations on $[\bar{2}\,11]$- and $[1\bar{1}0]$-misoriented surfaces, where surface faceting occurs simultaneously with the appearance of the (7×7) reconstruction at a temperature which decreases with increasing angle of misorientation.

## I. INTRODUCTION

The properties of vicinal, i.e., stepped, surfaces are of both practical and theoretical interest. Practically, stepped surfaces may serve as templates for improved epitaxial growth[1] or quantum wires.[2] Theoretically, atomic steps at surfaces may serve as physical realizations of statistical-mechanical models.[3] Unfortunately, little is known about the energetics governing the structure of steps on real surfaces. This problem is particularly difficult on surfaces which reconstruct, including most semiconductor surfaces. While theoretical understanding of the energetics of reconstructions is now becoming quantitative,[4] the addition of steps to the problem is still in exploratory stages.[5] In this paper we present low-energy electron diffraction measurements on vicinal Si(111) surfaces which show a clear relationship between step structure and surface reconstruction: we find that the "1×1"$\rightleftharpoons$(7×7) transition on Si(111) induces a tripling of the step height. When compared with previous results[6,7] on vicinal Si(111) surfaces containing steps of different orientation, these measurements show that this relationship is strongly dependent on step orientation.

It is not surprising that a relationship between step structure and reconstruction should exist: Although a detailed quantitative understanding is lacking, the step free energy will certainly depend on the presence or absence of a reconstruction. We have used this idea previously to explain the reversible faceting, which occurs upon passing through the "1×1"$\rightleftharpoons$(7×7) reconstructive phase transition,[6-8] of Si(111) vicinal surfaces misoriented towards the $[\bar{2}11]$ and $[1\bar{1}0]$ directions. These surfaces contain a uniform density of steps of height equal to the Si(111) double-layer spacing in the absence of the (7×7) reconstruction. The interaction of the (7×7) reconstruction with the steps on these surfaces is sufficiently unfavorable that beneath the reconstructive transition temperature these surfaces facet into unstepped reconstructed (111) regions and regions with a high density of steps and no ordered reconstruction. This reversible faceting was interpreted thermodynamically: in terms of the formation, at the "1×1"$\rightleftharpoons$(7×7) transition, of a sharp edge in the equilibrium crystal shape[9] of Si adjacent to the (111) facet.

The purpose of this work was to determine how steps on vicinal Si(111) surfaces misoriented toward a different azimuth, the $[2\bar{1}\,\bar{1}]$ direction, interact with the (7×7) reconstruction. To do this we have performed detailed low-energy electron diffraction (LEED) measurements to characterize the temperature dependence of the step structure for surfaces misoriented by 6° and 12° toward $[2\bar{1}\,\bar{1}]$. The possibility that reconstruction-induced changes in the configuration of steps on Si might depend on the step direction or azimuth of surface misorientation was suggested by reports in the literature[10-12] that surfaces misoriented toward $\langle 2\bar{1}\,\bar{1}\rangle$-type directions do not facet upon formation of the (7×7) reconstruction. If correct, this would indicate a strong dependence of the step-reconstruction interaction on the azimuthal direction of the step. For misorientations toward both the $\langle \bar{1}\,\bar{1}2\rangle$-type and $\langle \bar{2}11\rangle$-type directions, the step edges lie parallel to $\langle 1\bar{1}0\rangle$-type directions, as shown in Fig. 1. Since the (111) surface is threefold symmetric, the atomic geometry at the step edges is different for the two directions.[13] Scanning tunneling microscopy (STM) (Ref. 14) and low-energy electron reflection microscopy (LEERM) (Ref. 15) have shown formation of the reconstruction up to the step edges. Thus it is reasonable to anticipate that differences in step-edge structure could result in significantly different interactions with the (7×7) reconstruction.

The organization of this paper is as follows. In the

 

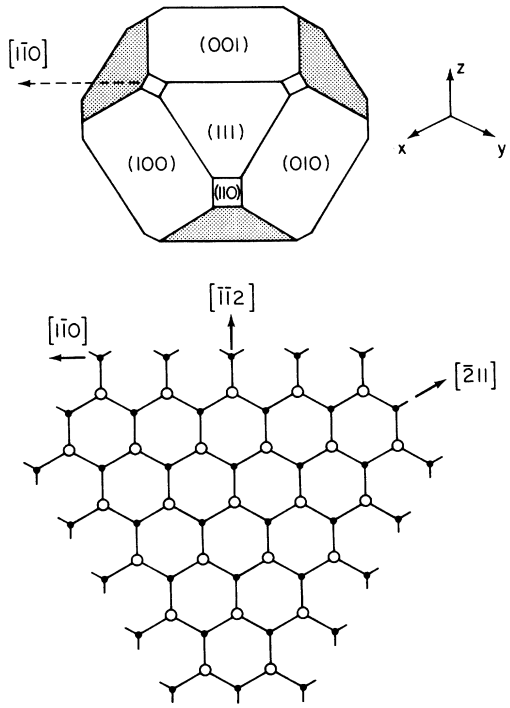


FIG. 1. Schematic of Si(111) surface in relation to other low index surfaces. The schematic of the bulk-terminated (111) surface in the lower panel is shown in the same orientation as the (111) face in the upper panel. Misorientation directions of the vicinal surfaces studied in this and previous work are indicated by arrows.

next section we briefly describe the experimental apparatus and procedures used in this study. We then present our results, consisting mainly of LEED angular profiles as a function of incident energy, as the temperature is lowered through the "(1×1)"⇌(7×7) reconstructive transition. Next, we discuss the nature of the structural transition and various possible structural models for the low-temperature step structure. We conclude by considering the significance of the qualitatively different results observed for vicinal Si(111) misorientations toward the [$\bar{2}$11] and [2$\bar{1}$ $\bar{1}$] directions.

## II. EXPERIMENT

Our experiments are performed in an ion-pumped stainless-steel vacuum system with a base pressure of $7\times10^{-11}$ mbar. Sample heating is by radiation and electron bombardment using a tungsten heater positioned behind the sample. Temperature is monitored with a W-5%Re versus W-26%Re thermocouple clamped to the edge of the sample, and calibrated against a disappearing filament pyrometer at temperatures where the sample is radiant.

In this study we have investigated two vicinal Si(111) orientations, misoriented by 6°, and by 12° toward an azimuth within a few degrees of [2$\bar{1}$ $\bar{1}$]. The doping of the samples was $n$ type, with a resistivity of 10–50 Ω cm. The surfaces were cleaned by heating to 1250 °C in ultrahigh vacuum for approximately 10 sec; the pressure in the system remained below $3\times10^{-10}$ mbar during these heatings. Surface composition was monitored using Auger electron spectroscopy. After heating to 1250 °C we were not able to detect any impurity peaks in the Auger spectrum, putting an upper limit of approximately $10^{-3}$ on the height of such a peak relative to the Si $LM_1M_2$ (92-eV) peak.

Our low-energy electron diffraction studies were performed by imaging the phosphor screen of a 4-grid LEED optics onto a vidicon tube. This system allows the diffracted intensity to be scanned along a given direction, and integrated along the orthogonal direction. The integration width along this orthogonal direction was typically chosen to be a few times the apparent full width at half maximum (FWHM) of the diffracted intensity peaks being imaged.

## III. RESULTS

### A. High-temperature step structure

Figure 2 shows the LEED pattern for a vicinal Si(111) surface misoriented by 6° toward [2$\bar{1}$ $\bar{1}$] at 870 °C, a temperature above that at which the $\frac{1}{7}$th-order reflections due to the (7×7) reconstruction of the Si(111) surface, disappear. At this incident angle and electron energy, certain of the integer-order reflections are split along the [2$\bar{1}$ $\bar{1}$] direction, as expected for a uniformly stepped surface and in agreement with previous reports.[11,12]

To obtain quantitative information about the surface step structure we measured angular profiles through various reflections as a function of the incident electron energy. As has been reviewed elsewhere,[16,17] the diffracted intensity from a regularly stepped surface ("staircase") is peaked along parallel line segments ("rods") in reciprocal space. The orientation of these rods is normal to the

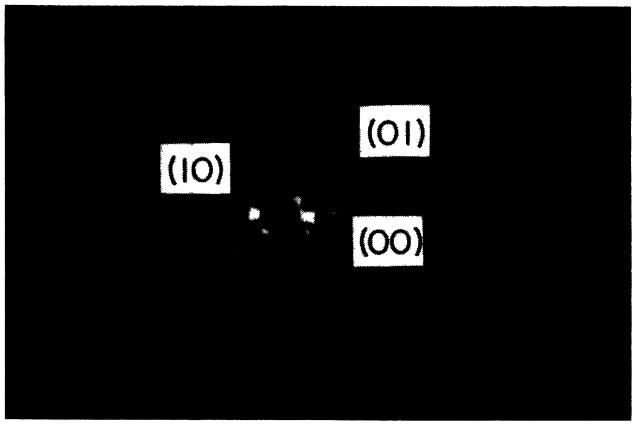


FIG. 2. LEED pattern for a vicinal Si(111) surface misoriented 6° toward [2$\bar{1}$ $\bar{1}$] at 870 °C. Incident energy = 48 eV. Incident angle = 10° with respect to [111]. Specular and first-order (111) reflections are indicated. First-order reciprocal-lattice vector is of magnitude $|a^*| = 1.889$ Å$^{-1}$

average stepped surface; the spacing of the rods is reciprocal to the staircase period.

Figure 3(a) shows diffracted intensity angular profiles through the (111) specular position, along the $[2\bar{1}\bar{1}]$ direction. The profiles were measured at a series of incident electron energies, at 870 °C. The abscissa shows the component of the momentum transfer within the (111) plane, $S_{\parallel}$. The offsets in the ordinate are proportional to the component of the momentum transfer perpendicular to the (111) plane, $S_{\perp}$, at the (111) specular position.[18] The extremes of the range for which data are shown, i.e., $S_{\perp}/S_{[111]} \simeq 3$ and 4, where $S_{[111]} \equiv 2\pi/d_{[111]}$, correspond to "in-phase" conditions for the specular reflection, for steps of height equal to the (111) interlayer spacing $d_{[111]}$. Here each profile consists of a single peak. For nonintegral values of $S_{\perp}/S_{[111]}$, each profile consists of two well-resolved peaks; these are symmetrically displaced from the specular position, and are approximately equally intense at $S_{\perp}/S_{[111]} \simeq 3\frac{1}{2}$, which corresponds to an "out-of-phase" condition for the specular beam for steps of height $d_{[111]}$.

Figure 3(b) shows the position of the intensity maxima of the component peaks, again in reciprocal space coordinates. These lie along parallel straight lines, which can be identified with two reciprocal lattice rods. The result of a least-squares fit of these positions to two parallel lines is shown in the figure. The slope of the lines is $0.102 \pm 0.004$; the spacing in $S_{\perp}$ between segments, at a fixed value of $S_{\parallel}$, is $2.12 \pm 0.10$ Å$^{-1}$. The fitted slope compares well with the tangent of the nominal 6° angle of misorientation, 0.105. Similar good agreement was obtained for the nominal 12° misorientation. The fitted period in $S_{\perp}$ is close to the bulk value of $2\pi/d_{[111]} = 2.004$ Å$^{-1}$. These results are consistent with a surface which contains a uniform density of steps of height close to the (111) interlayer spacing. In the following, for convenience in discussing our results, we will define an index for each split-component intensity peak, $n \equiv S_{\perp 0}/S_{[111]}$, where $S_{\perp 0}$ is the value of $S_{\perp}$ at which the corresponding reciprocal-lattice rod crosses the (111) specular position. As shown in Fig. 3(b) the fit yields $n \simeq 3,4$ (Ref. 18) for the two component peaks visible at high temperature.

### B. Temperature dependence of diffraction features

As the temperature of these surfaces is lowered through the "$(1\times1)$"$\rightleftharpoons(7\times7)$ reconstructive transition,

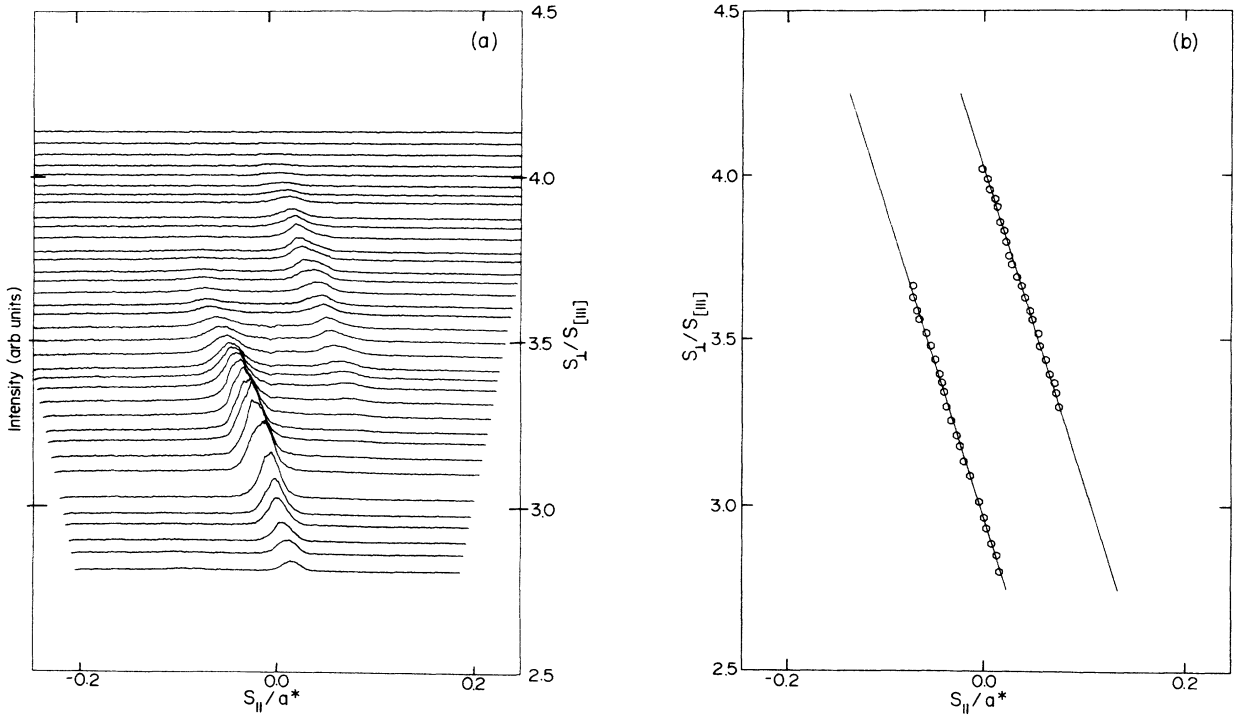


FIG. 3. (a) Angular profiles through the (111) specular position for surface misoriented by 6° toward $[2\bar{1}\bar{1}]$ at 870 °C. Horizontal coordinate is the component of the momentum transfer projected in (111) plane. Vertical offset, indicated at the left, is the component of the momentum transfer perpendicular to the (111) plane. Incident energies range from 31 eV at bottom to 67 eV at top, in steps of $\approx 1$ eV. Incident angle $= 10°$ with respect to [111]. $S_{\parallel}$ is measured in units of $|a^*|$, the bulk value of the Si(111) reciprocal mesh unit vector, equal in magnitude to 1.889 Å$^{-1}$; $S_{\perp}$ is expressed in units of $S_{[111]} \equiv 2\pi/d_{[111]}$ (i.e., in units of 2.004 Å$^{-1}$), where $d_{[111]}$ is the bulk Si(111) interlayer separation $d_{[111]} = 3.135$ Å. (b) Open circles show the positions of intensity component maxima in momentum transfer coordinates. Solid lines show the least-squares fit to parallel lines.

additional diffracted intensity peaks appear between those visible at high temperatures. As discussed below, this is indicative of a change in the step structure. Figure 4 shows the LEED pattern at 360 °C, well below the reconstructive transition temperature, again for a vicinal Si(111) surface misoriented by 6° toward $[2\bar{1}\,\bar{1}]$. Rather diffuse intensity peaks are seen at seventh-order positions in addition to the multiply split integer-order reflections. Diffuse streaks of intensity running along the $[2\bar{1}\,\bar{1}]$ direction are visible between reflections, those between the integer-order reflections being more intense. For the 12° misorientation, a similar pattern is observed; however, for this orientation a larger number of integer-order split components are visible, and the seventh-order reflections are considerably broader and dimmer.

Figure 5 shows in detail how the angular profiles of the diffracted intensity through the (111) specular position, measured at diffraction conditions close to $S_\perp/S_{[111]}=3\frac{1}{2}$, change as the temperature is lowered. The peaks visible at high temperature drop in intensity, and other peaks appear. In this figure the clearest signature of the change in step structure is the appearance of two additional peaks at positions approximately one-third of the way between the peaks observed at high temperatures; this is in agreement with earlier reports by Olshanetskii and co-workers.[11] The identification of these extra peaks with the $n\simeq 3\frac{1}{3}$ and $3\frac{2}{3}$ reciprocal lattice rods is confirmed by the energy dependence of the angular profile (as shown below, cf. Fig. 8) and indicates a tripling of the step period. Similar results are found for the 12° misorientation, i.e., intensity appears in the $n\simeq 3\frac{1}{3}$ and $3\frac{2}{3}$ positions over the same temperature range. However, for the 12° misorientation, the intensity in the $n\simeq 3$ and 4 positions does not decrease with decreasing temperature, as it does for the 6° misorientation.

To quantify the connection between the change in step structure with the appearance of the (7×7) reconstruction, Fig. 6 shows a comparison of the temperature dependence of the intensity at the positions of the $n\simeq 3\frac{1}{3}$ and $3\frac{2}{3}$ peaks with that of a seventh-order reflection (the seventh-order intensity is measured above a diffuse intensity background, taken as a straight line tangent to adjacent intensity minima in an angular profile). The $n\simeq 3\frac{1}{3}$ and $3\frac{2}{3}$ peaks and the seventh-order reflection appear at the same temperature. This temperature, as measured on multiple samples of each orientation, is 860±10 °C, and is the same for both the 6° and 12° misorientations to within the scatter in the determination. By contrast, in previous studies of vicinal Si(111) surfaces misoriented by 6° and 12° toward $[1\bar{1}0]$ the transition temperatures were 820 and 750 °C, respectively, a difference of 70 °C.[7]

The observed changes in the structure of the beam profiles, i.e., the number and spacing of peaks, are completely reversible with temperature. We have examined various ratios of the split-component peak intensities in attempting to characterize in detail the reversibility of the change in step structure. Figure 7 shows the temperature dependence of the ratio of the intensity measured at the position of the $n\simeq 3\frac{1}{3}$ peak to the intensity measured at the position of the $n\simeq 3$ peak, for successive cooling and warming experiments. The intensities are taken from angular profiles through the specular position, at an ener-

FIG. 4. LEED pattern for a vicinal Si(111) surface misoriented by 6° toward $[2\bar{1}\,\bar{1}]$ at 360 °C. Incident energy =48 eV. Incident angle =10° with respect to [111]. Reflection positions and scale as in Fig. 2.

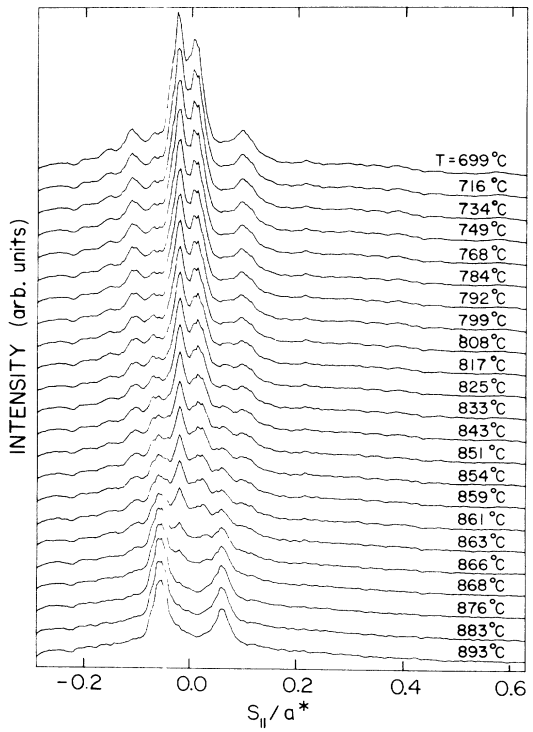


FIG. 5. Temperature dependence of angular profiles through the (111)-specular position near the $S_\perp/S_{[111]}=3\frac{1}{2}$ calculated out-of-phase condition. The two peaks observed at high temperature are the $n=3$ and 4 components. The intense peaks visible between these at low temperature are the $n=3\frac{1}{3}$ and $3\frac{2}{3}$ components. Incident energy =48 eV. Incident angle =10° with respect to [111].

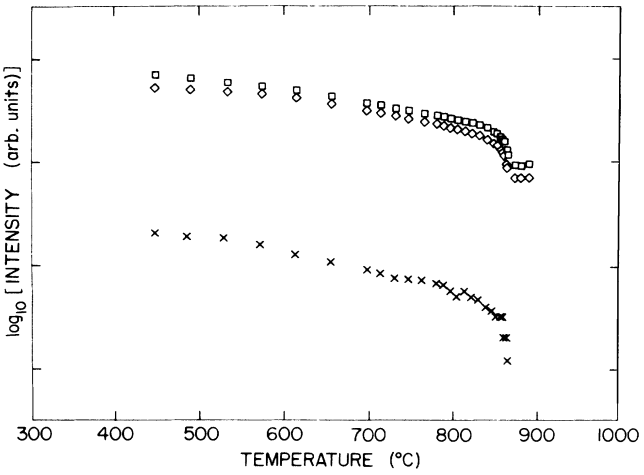


FIG. 6. Evidence that the change in step structure occurs coincident with the formation of the (7×7) reconstruction. The temperature dependences of the intensity at the positions of the $n=3\frac{1}{3}$ (squares) and $n=3\frac{2}{3}$ (diamonds) (111)-specular-beam intensity components, measured near $S_\perp/S_{[111]}=3\frac{1}{2}$ out-of-phase condition, are compared with that of the intensity of the $(\bar{3}/7\ 0)$ reflection (crosses) for a vicinal Si(111) surface misoriented 6° toward $[2\bar{1}\,\bar{1}]$. The specular-beam-component intensities are for an incident energy of 48 eV and incident angle of 10° with respect to [111]; the seventh-order intensities are for an incident energy of 43 eV and incident angle of 10° with respect to [111]. The seventh-order intensity is measured above a diffuse intensity background taken as a straight line tangent to adjacent intensity minima in the angular profiles.

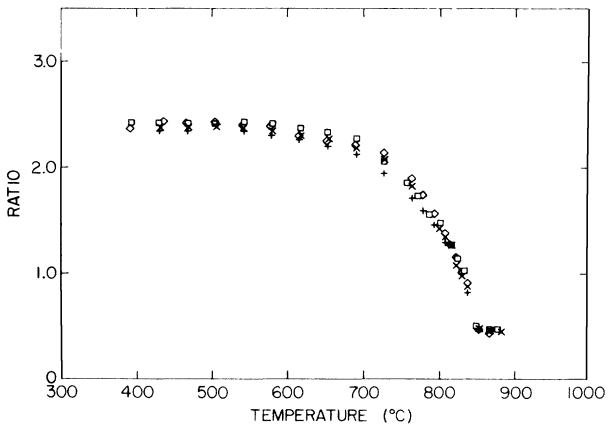


FIG. 7. Ratio of the intensity measured about the position of the $n=3\frac{1}{3}$ peak to the intensity about the position of the $n=3$ peak, in the (111)-specular beam profile; the measurements are for successive cooling (squares), heating (plus signs), cooling (diamonds) and heating (crosses). The intensities were measured near the $S_\perp/S_{[111]}=3\frac{1}{2}$ out-of-phase condition. The ratio is for a surface misoriented by 6° toward $[2\bar{1}\,\bar{1}]$. Incident energy =48 eV; incident angle of 10° with respect to [111]. Component intensities integrated over angular range spanning midpoints between adjacent component positions.

gy corresponding to $S_\perp/S_{[111]}\simeq 3\frac{1}{2}$. Results are similar for the ratio of the intensity measured at the position of the $n\simeq 3\frac{2}{3}$ peak to the intensity measured at the position of the $n\simeq 3$ peak. These ratios change sharply near $\simeq 860$ °C, and level off below $\simeq 600$ °C; they vary by approximately a factor of 5 over the temperature range shown. The ratios are very nearly reversible with temperature, with perhaps a slight tendency for the warming curves to be below the cooling curves. In addition, the structure observed at any temperature is independent of time: the shape of the beam profile does not change with time at any temperature, within our resolution, over times up to 120 min.

Although Fig. 7 shows convincingly that the step structure of the surface changes reversibly, it is difficult to draw conclusions about the reversibility of the entire state of the surface because of a monotonic drop of the intensities with time. The component peak intensities, measured at 900 °C, dropped by approximately 20% over the time interval during which the measurements of Fig. 7 were performed. Subsequent heating of the surface to 1250 °C resulted in a recovery of the original intensities. A fit of the time dependence to an exponential decay yields a time constant of roughly 3 h at 900 °C. This time constant is quite insensitive to the ambient pressure; turning off the ion pump produced a pressure rise into the $10^{-8}$-mbar range over the course of 2 h, but produced no observable change in the time dependence of the intensity from that measured at a pressure of approximately $10^{-10}$ mbar. Measurements performed at temperatures between 300 and 900 °C revealed a strong, monotonic increase of this time constant with decreasing temperature; at temperatures below 500 °C the drop in intensity after 2 h is less than the uncertainty in the determination. We do not detect changes in the peak splitting or component peak widths with time at any temperature. Measurements of Auger electron spectra failed to indicate the presence of any impurity peak, even after $2\frac{1}{2}$h at 900 °C. A reexamination of our data for surfaces misoriented toward the $[\bar{2}11]$ and $[1\bar{1}0]$ directions[7] indicates that a similar monotonic drop in the intensity of the reflections from the stepped parts of these surfaces occurs for these misorientations as well, although the temperature dependence of the peak splittings is reversible, to within our resolution. A decrease in the ordered surface area due to sublimation from defect sites is a possible explanation of these observations.[19–21]

### C. Low-temperature step structure

To determine the low-temperature step structure, we again measured the energy dependence of angular profiles through (111) integer-order positions. The energy dependence of the diffracted intensity in the vicinity of the (111) specular position at a temperature 200 °C below the appearance of the seventh-order reflections is shown in Fig. 8(a). Similar results are observed in profiles measured in the vicinity of the other (111) integer-order reflections. The data are again plotted in momentum-transfer coordinates, over the same range of incident energies as for Fig. 3. Four intense component peaks are

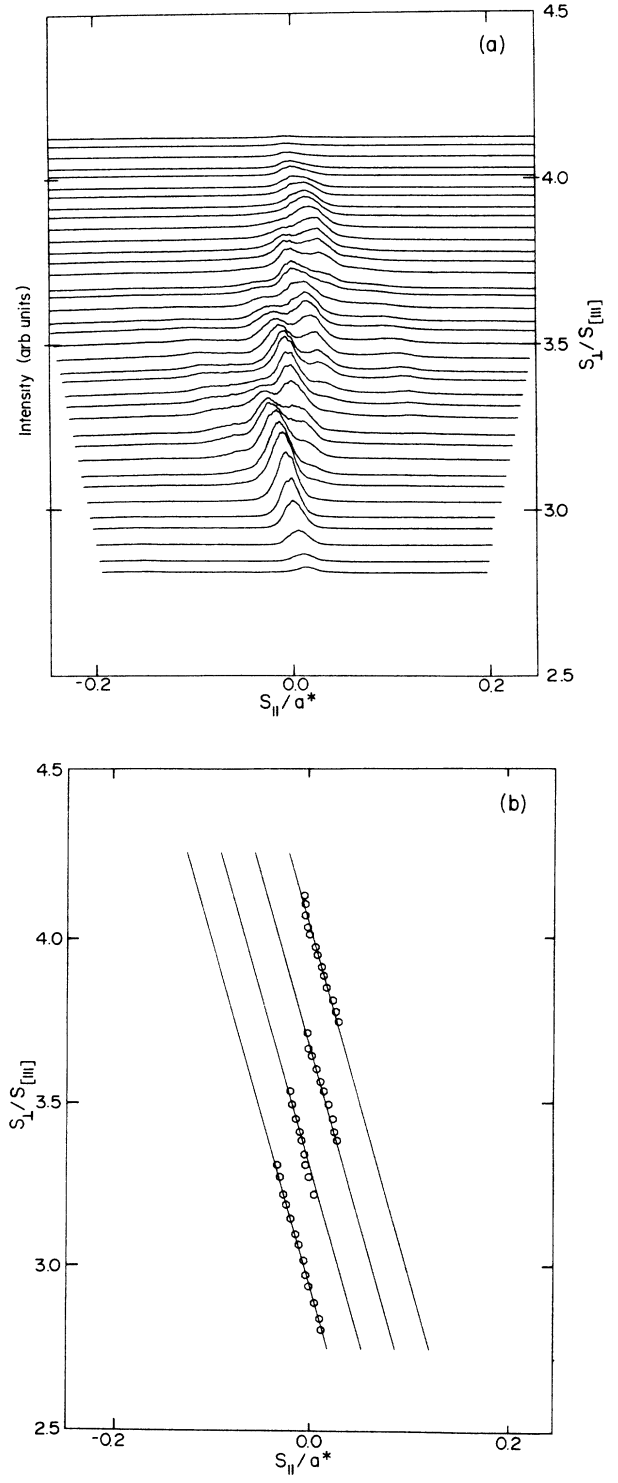


FIG. 8. (a) Angular profiles through the (111)-specular position for surface misoriented by 6° toward $[2\bar{1}\,\bar{1}]$ at 660 °C. Coordinates as in Fig. 3. Incident energies range from 31 eV at bottom to 67 eV at top, in steps of ≈1 eV. Incident angle of 10° with respect to [111]. The expansion of the horizontal axis and compression of the vertical scale cause the apparent difference with the low-temperature profiles of Fig. 5. (b) Open circles show positions of the four most intense component-peak maxima in momentum transfer coordinates. Solid lines show the least-squares fit to parallel, equally spaced lines.

visible within the range of energy for which data are shown. An additional pair of weak component peaks (more readily seen in Fig. 5) are visible over a narrow energy range. These component peaks are broad, and overlap both the $n=2\frac{1}{3}$ and $2\frac{2}{3}$ positions on the low $S_\parallel$ side and the $n=4\frac{1}{3}$ and $4\frac{2}{3}$ positions on the high $S_\parallel$ side. In contrast to results[7] for misorientations toward $[\bar{2}11]$ and misorientations toward or away from $[1\bar{1}0]$, there is no sign of a peak which remains at the specular position (i.e., $S_\parallel=0$) as the energy (and thus $S_\perp$) is varied. Figure 8(b) shows the positions of the component peak intensity maxima. Once again the positions tend to lie along roughly parallel lines in reciprocal space. Separate least-squares fits to the positions of each of the component peaks yielded slopes which varied from each other by approximately ±10%; this scatter might be due to the restricted range in energy over which it was possible to determine each of the individual peak positions, making it difficult to average out the effects of imaging the diffraction through crossed grids. Figure 8(b) shows a fit of the positions of the four intense components visible in Fig. 8(a) to parallel, equally spaced line segments in reciprocal space. The reciprocal lattice rod indexes associated with these intensity components are $n\simeq 3$, $3\frac{1}{3}$, $3\frac{2}{3}$, and 4. The slope is 0.092±0.008, which, to within the calculated uncertainty in the fit, is unchanged from the high-temperature value of 0.102±0.004. The spacing of the lines in $S_\perp$ is 0.72±0.08 $\text{Å}^{-1}$, somewhat larger than $2\pi/3d_{[111]}=0.608$ $\text{Å}^{-1}$; however, the ratio of the fitted low-temperature to high-temperature spacings is 1:2.94±0.35. These results are consistent with a tripling of the step period and height, preserving the net angle of misorientation for both the 6° and 12° samples.

However, as discussed in the next section, and shown in detail in the Appendix, the intensity distribution among the split components is not as expected for simple triple-height steps on the basis of the kinematic approximation (cf. Fig. 10). In particular, the observation of more than one peak in the beam profiles at the triple-height step in-phase conditions ($S_\perp/S_{[111]}=3\frac{1}{3}$ and $3\frac{2}{3}$) indicates that the step-period tripling involves a more complex step structure. In an attempt to investigate whether the observed distribution of intensities is due to multiple-scattering effects, we have performed measurements over a range of incident directions, with the incident azimuth [i.e., the projection of the incident electron momentum in the (111) plane] parallel to [211] at right angles to $[2\bar{1}\,\bar{1}]$ and along a number of intermediate azimuths. For all of the incident directions we have investigated, we observe qualitatively similar $S_\perp$ dependences for angular profiles through the integer-order reflections. In particular, multiple component peaks are observed at calculated out-of-phase conditions for steps of height equal to $d_{[111]}$ (e.g., for the specular beam, at $S_\perp/S_{[111]}=m+\frac{1}{2}$, with $m$ an integer), and single narrow reflections at calculated in-phase conditions for steps of this height (for the specular beam, $S_\perp/S_{[111]}=m$), but multiple component peaks at additional calculated in-phase conditions for steps of height $3d_{[111]}$ (for the specular beam, $S_\perp/S_{[111]}=m\pm\frac{1}{3}$). Since within a multiple-

scattering description the diffracted intensity depends not only on the momentum transfer but on the incident direction as well,[22] this is an indication that the anomalous number of split peaks in the measured beam profiles might not be due to multiple scattering.

Although it is difficult to discern, due to the coordinate system used[23] for Figs. 3 and 8, the split components of the integer-order reflection show a slight broadening at out-of-phase conditions, indicating some disorder.[24–26] Further indications of this are finite intensity at $S_{\parallel}=0$ in the high-temperature specular-beam profiles, and the streaks of intensity running along the $[2\bar{1}\,\bar{1}]$ direction between reflections in the low-temperature diffraction pattern. The seventh-order reflections also show a broadening along the $[2\bar{1}\,\bar{1}]$ direction. We have not been able to resolve a periodic splitting, or broadening and narrowing, of these reflections along this direction as the incident electron energy is varied; this suggests that the domains of (7×7) reconstruction are not correlated across step edges. For the 6° misoriented surface the broadening of the seventh-order beams beyond the instrument limit corresponds to a domain size of between 20 and 50 lattice spacing;[27] this is to be compared with a terrace width of 24 spacings, or slightly more than three (7×7) unit cell widths, for a uniformly stepped surface containing steps of height $3d_{[111]}$.

## IV. DISCUSSION

Our results show that a tripling of the step period occurs coincident with the formation of the (7×7) reconstruction, in agreement with earlier observations.[11] The transition occurs over a narrow temperature range ($\Delta T \simeq 0.03 T_c$). Most remarkably, the transition temperature is independent of the angle of misorientation to within ±10 °C up to 12° misorientation.[28] These results are in distinct contrast to those[7] for surfaces misoriented toward the $[\bar{2}11]$ and $[1\bar{1}0]$ directions. For those surfaces the "1×1"⇌(7×7) reconstruction transition temperature is depressed with increasing angle of misorientation, and the appearance of the (7×7) reconstruction is coincident with a faceting of the surface.

The striking difference in the temperature dependence of the step structure of vicinal Si(111) surfaces misoriented towards the $[\bar{2}11]$ and $[2\bar{1}\,\bar{1}]$ directions is at first sight surprising considering observations by scanning tunneling microscopy[14] that the placement of the (7×7) reconstruction relative to either type of step is similar. Indeed, the presence of both stacking faulted and unfaulted regions of the unit cell in the currently accepted dimer–adatom–stacking-fault (DAS) model[29] of the (7×7) reconstruction results in the top double layer of atoms being quasisixfold symmetric. However, a stepped (111) surface contains a number of exposed double layers, and the threefold symmetry of the underlying bulk is therefore important. For the DAS reconstruction a consequence of this oddfold symmetry, illustrated in Fig. 9, is that $[\bar{2}11]$-type step edges require a defect in the reconstruction, in the form of a missing dimer chain after a step; $[2\bar{1}\,\bar{1}]$-type edges do not.

Additional experimental evidence for a strong

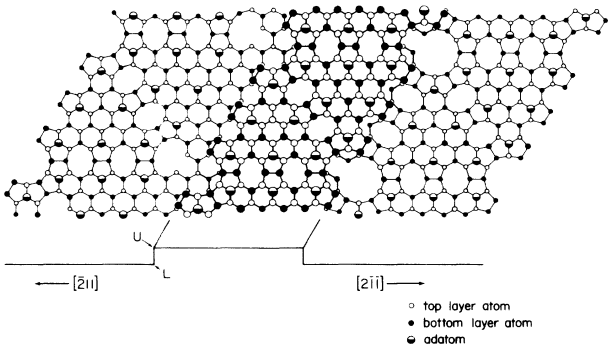


FIG. 9. Dimer–adatom–stacking-fault (DAS) (7×7) reconstructed (111) terrace bounded by steps of $\langle\bar{2}11\rangle$ and $\langle 2\bar{1}\,\bar{1}\rangle$ type. "*U*" indicates upper or outer edge of rise. "*L*" indicates lower or bottom edge of riser.

difference between the nature of the interaction of the reconstruction with $[\bar{2}11]$ and $[2\bar{1}\,\bar{1}]$ step edges has been provided by the study of Telieps and Bauer[30] of the nucleated growth of the (7×7) reconstruction at steps. They show that the (7×7) domains are triangular and appear with an edge preferentially aligned with the top edges of steps misoriented toward the $[2\bar{1}\,\bar{1}]$ direction, and with a truncated apex aligned with steps directed toward the $[\bar{2}11]$ direction.

The observed reversibility of the step-height tripling for vicinal Si(111) misorientations toward $[2\bar{1}\,\bar{1}]$, and of the faceting of vicinal misorientations toward $[\bar{2}11]$ and $[1\bar{1}0]$ is consistent with thermodynamic driving forces for both of these transformations. Previously, we interpreted the faceting of the misorientations toward $[\bar{2}11]$ and $[1\bar{1}0]$ as due to a very high free-energy "cost" for steps on the (7×7)-reconstructed surface compared to steps on the "1×1" surface.[7,8] In this model, the free-energy cost is responsible for lowering the temperature at which the (7×7) reconstruction forms with increasing net density of steps; for the surface misoriented by 12° toward $[1\bar{1}0]$ the reconstructive transition is depressed by approximately 100 °C below that on the singular surface. The lack of analogous behavior for the $[2\bar{1}\,\bar{1}]$-misoriented surfaces would suggest that for this step orientation the difference in the free-energy cost for steps on the reconstructed and unreconstructed surfaces is small.[8]

Although the reversibility of the transition between the two step structures is consistent with a thermodynamic driving force for the transition, it does not rule out that changes in step structure might be driven by changes in kinetic processes such as sublimation and anisotropic diffusion across step edges.[31,32] The coincidence of the reconstructive transition and the step tripling indicates that if such processes are important in determining the step structure the formation of the (7×7) reconstruction must play a strong role, and thus energetics would still indirectly drive the transformation. Similar arguments apply to a description of the faceting observed[6,7] on misorientations toward $[\bar{2}11]$ and $[1\bar{1}0]$. As it is known[15,33] that the reconstruction nucleates at step edges, it is quite reasonable that the reconstructive transi-

tion could change the rates of kinetic processes occurring at step edges. An indication that the step tripling might be driven by changes in kinetic processes, and not entirely by energetics, is a recent suggestion based on the scanning tunneling microscopy observation that the triple-height structure might not be stable at temperatures well below the "1×1"⇌(7×7) transition.[34]

An understanding of the reason for the preference for the triple-layer height steps on the surface upon lowering the temperature through the reconstructive transition would require a knowledge of the configuration of atoms at the step edges. We have performed kinematical beam profile calculations for a number of simple structural models of the low-temperature surface, and present the results in the Appendix. We have found no simple structure which quantitatively reproduces all of the details of our beam profiles. However, our measurements allow us to rule out the simplest triple-height structure, in which risers of height $3d_{[111]}$ and (100) orientation separate (111) terraces. This triple-period structure produces very nearly a simple factor of 3 decrease in the scale of the reciprocal space period, and does not explain the observed qualitative differences in profiles measured at different in-phase conditions (e.g., for the specular beam, profiles consisting of single peaks at $S_\perp/S_{[111]}=3$ and 4, but asymmetric multiple-peak profiles at $S_\perp/S_{[111]}=3\frac{1}{3}$, $3\frac{2}{3}$, cf. Fig. 10). Alternative, more complex models include structures in which steps of height $d_{[111]}$ separate terraces whose widths vary with a period of three terraces, and structures in which regions containing steps of height $3d_{[111]}$ coexist with regions containing steps of height $d_{[111]}$.[34] Such models produce qualitative agreement with some features of the observed beam profiles, as can be seen in the Appendix. Quantitative agreement might be possible by variation of structural parameters within these models. However, questions of uniqueness, and the limitations of the kinematical model in describing relative peak intensities in LEED, would make the resulting structural determination unreliable.

Despite the lack of a detailed structural model for the step-edge configuration, some general remarks can be made about the cause of the step-height tripling, based on our LEED observations. Because the observed change in step height seems to be primarily determined by the reconstructive transition and not the properties of steps, theories[3] of transitions between steps of multiple-layer height caused by the increased entropy due to step wandering do not seem to be applicable here. In contrast to the strongly angle-dependent faceting temperature observed for the misorientations toward $[\bar{2}11]$ and $[1\bar{1}0]$, the step-height tripling temperature is independent of misorientation for angles of up to 12°. This independence suggests that although the step structure changes during the reconstructive transition, the step configuration itself plays little role in determining the transition temperature. That is, the step structure changes because of the change in reconstruction, but the steps have little effect on the driving force for the (7×7) to "1×1" transition. This is noteworthy because our diffraction measurements show that the steps severely limit the range of the (7×7)-order perpendicular to the steps.

## V. CONCLUSIONS

On vicinal surfaces misoriented toward the high-symmetry $[2\bar{1}\,\bar{1}]$ direction we observe a step-period tripling on lowering the temperature through the reconstructive transition temperature. The number and relative intensities of peaks in beam profiles kinematically calculated for the simplest triple height steps which might exist on the surface are not consistent with the observed LEED pattern. This might be due to limitations of the kinematic model. However, addition of three-dimensional structure to the tripled-period unit cell can cause qualitatively similar changes in intensity, within the kinematic model. There are a number of more complex triple-period structures possible for the low-temperature triple-period phase, and a unique determination cannot be made by comparison with the data. The coincidence of the reconstructive transition temperature and that at which the period changes suggests that the placement of the reconstruction relative to the step edges is important in this structure.

The observed transition from a uniform vicinal surface for the high-temperature "1×1" surface to a triple-period uniform vicinal surface for the low-temperature (7×7) reconstructed surface is reversible with temperature, upon warming and cooling, and occurs in a narrow temperature range exactly coincident with that of the "1×1"⇌(7×7) transition. The transition temperature is the same for both 6° and 12° misorientations, to within the uncertainty of the determination. The nature of the transition is qualitatively different from the faceting observed on misorientations toward the $[\bar{2}11]$ and $[1\bar{1}0]$ directions. This indicates a strong dependence of the step-reconstruction interaction on the step orientation. This conclusion holds whether the driving force is thermodynamic or kinetic in origin.

## ACKNOWLEDGMENTS

We wish to thank T. Jung for his help in some of the data acquisition and analysis, and N. C. Bartelt for many useful discussions. We thank the Laboratory for Physical Sciences (University of Maryland) for providing the facilities with which these experiments were performed. This work was funded by the U.S. Department of Defense (DoD) and Office of Naval Research (ONR) under Research Grants No. N00014-86-K-0627 and No. N00014-86-K-0328.

## APPENDIX

Simple kinematical calculations of the diffracted interference function[35] in the vicinity of the (111) specular position were performed for a number of possible models for a triple-oriented step structure. The calculations are over approximately the same ranges of the parallel and perpendicular components of momentum transfer as the measured beam profiles of Fig. 8. Neglecting a small variation in $S_\perp$ for the measured profiles, a direct comparison can be made. A more detailed comparison would require convolving the calculated profiles with an instrument response function.[36] Because of problems with

uniqueness in a system with so many parameters, and the neglect of dynamical effects in the calculation, the purpose of this section is not to make a step-structure determination from the data. Instead, the aim is to show that the anomalous profiles observed experimentally are consistent with a triple-period structure. Table I lists structural models for which LEED beam profiles were calculated, and summarizes the results. This list is not exhaustive, but does include models previously proposed[11,12] for the low-temperature step structure, as well as some other simple possibilities.

### 1. Periodic step structures

In this section we consider structures which can be decomposed into a "staircase" lattice, with a period along [111] of $3d_{[111]}$, and a basis, i.e., the arrangement of surface atoms between adjacent lattice points, which might contain steps of various heights. The calculated specular-beam profiles presented in Figs. 10–13 consist of the product of two factors. The first is the form factor, corresponding to the scattering from a single basis. Because of the finite size of the basis, the form factor gives

TABLE I. Summary of features of observed and calculated specular beam profiles, at triple-height in-phase conditions ($S_\perp/S_{[111]}=3\frac{1}{3}$ and $3\frac{2}{3}$) and out-of-phase condition ($S_\perp/S_{[111]}=3\frac{1}{2}$). In this table "in-phase" indicates a peak at the specular position; "out-of-phase" indicates no peak at the specular position, but two peaks symmetrically displaced from this position. For $S_\perp/S_{[111]}=3\frac{1}{3}$ and $3\frac{2}{3}$ the term "side peaks" indicates peaks away from the specular position; for $S_\perp/S_{[111]}=3\frac{1}{2}$ this term indicates peaks outside those closest to the specular position (i.e., outside those corresponding to the $n=3\frac{1}{3}$ and $3\frac{2}{3}$ rods, e.g., the $n=3$ and 4 rods). Relative observed side-peak intensities or calculated values of the interference function (Ref. 35) are described with respect to the in-phase peak for $S_\perp/S_{[111]}=3\frac{1}{3}$ and $3\frac{2}{3}$, and with respect to the $n=3\frac{1}{3}$ and $3\frac{2}{3}$ peaks for $S_\perp/S_{[111]}=3\frac{1}{2}$. "Strong" indicates a relative intensity greater than or equal to 1. "Weak" indicates a relative intensity of between 0.1 and 0.01. "Very weak or missing" indicates a relative intensity of less than 0.01. "Asymmetric" indicates that the most intense side peaks on opposite sides of the specular position have intensities which differ in relative intensity by a factor of 1.5 or more, or that there are a larger number of intense side peaks on one side of the specular position. "Multiple" indicates more than one intense side peak on one side, or on both sides, of the specular position.

| Model | $S_\perp/S_{[111]}=3\frac{1}{3},3\frac{2}{3}$ | $S_\perp/S_{[111]}=3\frac{1}{2}$ |
|---|---|---|
| Observed (Fig. 8) | in-phase, asymmetric side peaks | out-of-phase, symmetric, multiple side peaks |
| Periodic $3d_{[111]}$ no 7×7 (Fig. 10) | in-phase, very weak or missing side peaks | out-of-phase, symmetric, weak side peaks |
| Periodic $3d_{[111]}$ correlated 7×7 | in-phase, weak side peaks | out-of-phase, asymmetric side peaks |
| Periodic $2d_{[111]}+d_{[111]}$ 6°, no 7×7 | in-phase, symmetric, strong side peaks | out-of-phase, symmetric side peaks |
| Periodic $d_{[111]}$ 6°, no 7×7 | in-phase, asymmetric, multiple side peaks | out-of-phase, symmetric, multiple weak side peaks $n=3,4$ side peaks very weak or missing |
| Periodic $d_{[111]}$ 6°, correlated 7×7 | in-phase, asymmetric, multiple side peaks | out-of-phase, symmetric, multiple side peaks, $n=3,4$ side peaks weak |
| Periodic $d_{[111]}$ 12°, no 7×7 (Fig. 11) | in-phase, asymmetric, multiple strong side peaks | out-of-phase, symmetric, strong side peaks |
| Periodic $d_{[111]}$ 12°, correlated 7×7 (Fig. 12) | in-phase beam weak or very weak, asymmetric, multiple strong side peaks | out-of-phase, $n=3\frac{1}{3},3\frac{2}{3}$ peaks weak symmetric, multiple strong side peaks |
| Coexistence of $3d_{[111]}+d_{[111]}$ (Fig. 13) | in-phase, asymmetric side peaks | out-of-phase, symmetric side peaks |
| Random mixture of $2d_{[111]}+d_{[111]}$ | near out-of-phase, spacings wrong | variable with mixture, peaks broadened |
| Random mixture of $3d_{[111]}+d_{[111]}$ | variable with mixture: near in-phase for mostly $3d_{[111]}$, spacings right for mostly $3d_{[111]}$, peaks broadened | out of phase |

rise to broad profiles, which are shown by dotted lines in the figures. The second factor gives rise to a set of $\delta$-function-width "rods" in reciprocal space, which are inclined with respect to [111] by the staircase angle, and are spaced along $[2\bar{1}\,\bar{1}]$ by $\Delta S_{\parallel}=2\pi/A_{\parallel}$, where $A_{\parallel}$ is the component of the separation between adjacent staircase lattice points along $[2\bar{1}\,\bar{1}]$ (i.e., the spacing is reciprocal to the staircase periodicity). The resulting interference function profiles are shown by a set of vertical line segments.

The calculations for these models include contributions from identical scatterers located in the atomic positions in the top Si(111) double layer only. To investigate how large an effect the (7×7) reconstruction has on the calculated profiles, we have considered two extreme cases. In the first case, the reconstruction is neglected, and the scatterers are arranged in bulk Si(111) atomic positions. In the second case, on the reconstructed parts of the surface the scatterers are arranged according to the dynamical LEED optimized[37] DAS (7×7) model (including adatoms); on the remaining parts of the surface the scatterers are arranged in bulk Si(111) atomic positions (with no adatoms included). The first case might approximate a structure on which the position of the reconstruction on successive reconstructed terraces is entirely uncorrelated. The second case represents a perfect positional correlation between reconstructed terraces.

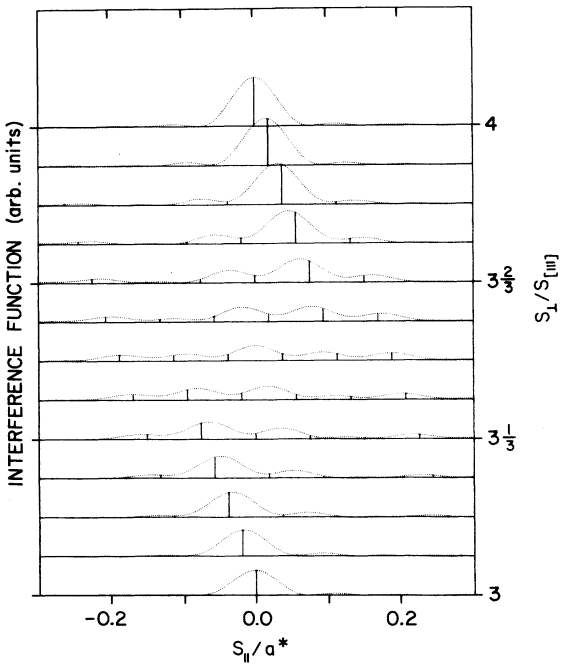


FIG. 11. Calculated specular beam profiles for a vicinal surface containing steps of height $d_{[111]}$, and unreconstructed (111) terraces of modulated width. Period of modulation is three terraces. Basis contains a terrace seven Si(111) bulk lattice spacings wide alternating with pairs of terraces two spacings wide. Terrace widths correspond to staircase angle of 12°.

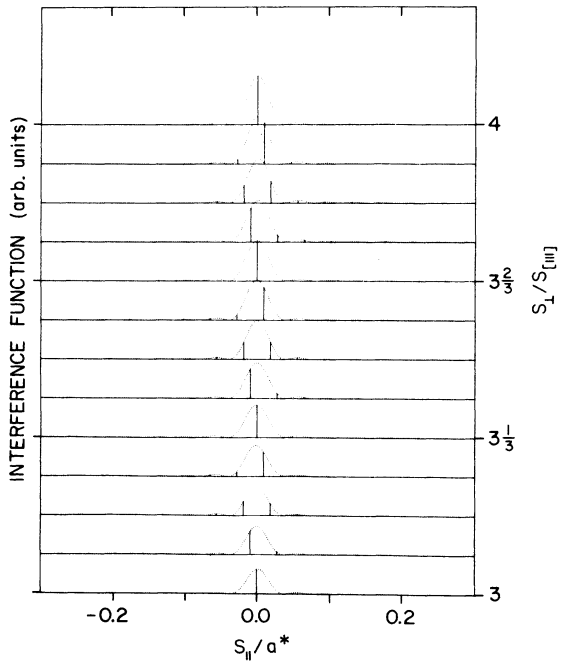


FIG. 10. Calculated kinematic specular beam profiles for a vicinal surface containing steps of height $3d_{[111]}$ and unreconstructed (111) terraces. Form factors are shown by dotted curves. Beam profiles consist of narrow peaks, indicated by vertical line segments. Terrace width of 25 Si(111) bulk lattice spacings corresponds to a staircase angle of 6° (see text for details of basis).

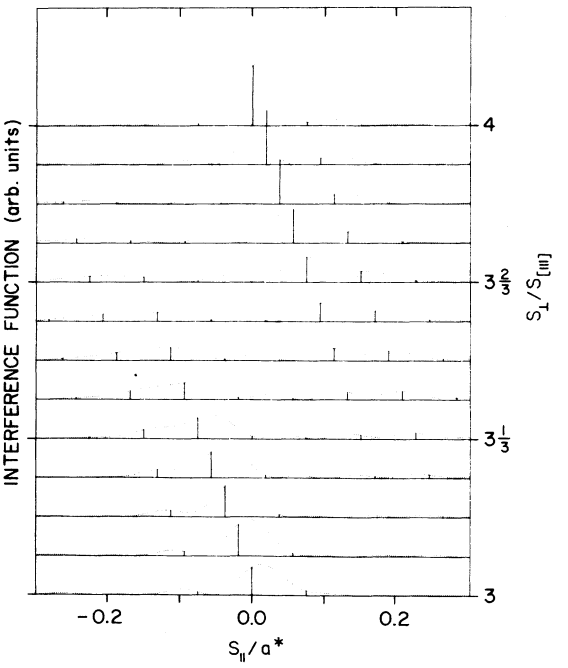


FIG. 12. Calculated specular beam profiles for a vicinal surface containing steps of height $d_{[111]}$ and a DAS (7×7) unit cell on every third terrace. Terrace widths and staircase angle as in Fig. 11.

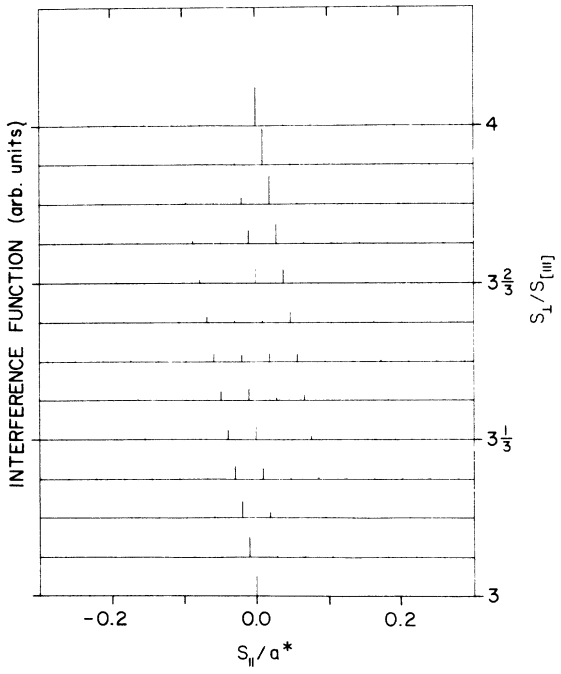


FIG. 13. Calculated specular beam profiles for a vicinal surface composed of coexisting, positionally uncorrelated regions containing steps of height $3d_{[111]}$, and regions of height $d_{[111]}$. The form factors, which are different for the two types of regions, are omitted for clarity. The staircase angle for both types of regions is 6°.

### *a. Steps of height $3d_{[111]}$*

Figure 10 shows the result for a surface on which risers of height $3d_{[111]}$ and of (100) orientation separate terraces of (111) orientation, 25 spacings wide, corresponding to a misorientation angle of 6°. Over the same range in $S_\perp$ as in Fig. 8, the shape of the calculated form factor varies little, and yields significant intensity only near the specular position, with essentially zero intensity at $S_\parallel = \pm 2\pi / A_\parallel$. The calculation was repeated with the terrace atoms arranged in the positions of three adjacent (7×7) unit cells, with a dimer chain placed against the $[2\bar{1}\,\bar{1}]$ upper step edge, and an unreconstructed region four spacings wide adjacent to a lower step edge. The form factor in this case yields some weak intensity away from the integer-order beam position, but still does not account for the large relative intensity observed in side peaks at in-phase and out-of-phase conditions for steps of height $3d_{[111]}$.

### *b. Steps of $2d_{[111]}$ and $d_{[111]}$*

A stronger variation in the form factor with $S_\perp$ occurs for triple-period structures in which the basis contains a group of steps. Previous workers[12] proposed that these surfaces contain a mixture of steps of height $2d_{[111]}$ with steps of height $d_{[111]}$; here we consider an ordered grouping of steps of these two heights. Calculations were performed for this model for terraces of a single width, containing scatterers arranged in bulk Si(111) atomic positions, and separated by alternating risers of height $2d_{[111]}$ and $d_{[111]}$. The calculated beam profiles at in-phase conditions for steps of height $3d_{[111]}$ show a peak at the specular position, as well as two symmetrically displaced, equal-intensity side peaks, in contrast to the asymmetry visible in Fig. 8.

### *c. Steps of height $d_{[111]}$ only*

There are many ways to generate a grouping of three steps of height $d_{[111]}$ separating terraces of different widths, however the small step separation on surfaces misoriented by 12° toward $[2\bar{1}\,\bar{1}]$ limits the number of models involving the (7×7) reconstruction. (Triple-period step structures containing only steps of height $d_{[111]}$ separating terraces, each of which is seven or more spacings wide, are not possible on a uniformly stepped surface misoriented by an angle greater than 7.0°; structures containing only steps of height $d_{[111]}$ separating terraces, two-thirds of which are seven or more spacings wide, are not possible on a uniform surface misoriented by an angle greater than 10.0°.) An example of this type of structure has every third terrace width equal to the (7×7)-unit-cell width times the maximum integer consistent with the misorientation angle, and the widths of the intervening two terraces adjusted to make up the misorientation. Such a basis, for a 6° misorientation, includes terraces 21 spacings wide alternating with pairs of terraces, each two spacings wide. The beam profiles were calculated for both 6° and 12° orientations, both with and without the (7×7) reconstruction. The results showed a trend to better agreement with the observed profiles than those discussed above. In particular, an asymmetry in the side peaks near triple-height step in-phase conditions is qualitatively reproduced in the calculated profiles. This is more pronounced for the 6° misorientation in the presence of the (7×7) reconstruction. However, for the 12° misorientation,[38] inclusion of the (7×7) reconstruction greatly reduces the extent of the agreement with the observed profiles. The calculated curves for the 12° misorientation, with and without the (7×7) reconstruction, are shown in Figs. 11 and 12.

### 2. Coexisting periodic stepped phases

By "coexisting phases," in this context we mean the existence of patches of different step structure on the surface, with each patch large compared to the staircase period, and with relative patch placements not correlated. The resulting diffracted interference function is the sum of that from each patch, or domain. The only simple coexistence of regions of regular structures which might produce in phase condition beam profiles consistent with our observations would be domains containing steps of height $3d_{[111]}$ and domains containing steps of height $d_{[111]}$. The relative intensities of the two sets of reflections depend on the sizes and relative numbers of each domain. Figure 13 shows calculated specular-beam profiles for a simple illustrative case,[39] with both types of domain contributing equally at the in-phase positions. Since the orientations of the two types is the same, the

$n=3$ and 4 peaks from patches of the two step heights overlap. The profiles consist mainly of four intense split components corresponding to $n=3$, $3\frac{1}{3}$, $3\frac{2}{3}$, and 4. In addition, the $n=3$ and 4 component peaks are quite prominent in the calculated profile at the $S_\perp/S_{[111]}=3\frac{1}{2}$ out-of-phase condition, which is not observed experimentally for the 6° misorientation, but is observed for the 12° misorientation.

### 3. Uncorrelated mixtures of step heights

Calculations of interference function beam profiles for step structures containing an uncorrelated mixture of different step heights can be performed approximately, as considered previously.[24–26] The analysis is two dimensional, i.e., the steps run along a single direction. Effects due to reconstruction of the terraces and contributions to the scattering from riser atoms are not included. The risers we have considered are of the simplest type for misorientations toward $[2\bar{1}\,\bar{1}]$, and have orientation [100] resulting in reciprocal unit mesh vectors which are not orthogonal. In the calculation, the momentum transfer for each calculated profile was varied along a direction parallel to $[2\bar{1}\,\bar{1}]$ (i.e., the components along both reciprocal unit mesh vectors were varied simultaneously) to allow for direct comparison with the measured beam profiles of Fig. 8.

#### a. *Steps of height $2d_{[111]}$ and $d_{[111]}$*

This model was suggested in Ref. 12 to explain poorly resolved integer-order LEED beam splittings for vicinal misorientations toward $[2\bar{1}\,\bar{1}]$ at temperatures below the appearance of the $(7\times7)$ reconstruction (this is in contrast to our observations of well-resolved beam splitting, shown for the specular beam in Fig. 8). The step-height distribution is taken to be the sum of two $\delta$ functions of strength $h_1$ and $h_2$, where $h_1+h_2=1$. For simplicity, we include only a single terrace width in the structure, $L_A$, which is taken to be consistent with the angle of misorientation and the average step height $h_A=(h_1d_{[111]}+2h_2d_{[111]})/(h_1+h_2)$. The disorder in the step heights produces a broadening of the calculated peaks, and a departure of the peak positions from straight lines in reciprocal space, near $S_\perp/S_{[111]}=n+\frac{1}{2}$ (i.e., near single-height step out-of-phase conditions). This effect is maximal for an equal fraction of steps of height $d_{[111]}$ and $2d_{[111]}$, where it results in a coalescing of split beams into a single broad (FWHM$=2\pi/L_A$) peak at the specular position at the out-of-phase condition.

A comparison of the calculated profiles with those of Fig. 8 yields poor agreement for any choice of the relative fractions of the two step heights. In particular, for calculated profiles in which split beams are resoled, the spacing in $S_\parallel$ between adjacent peaks is not $2\pi/3L_A$, as expected (cf. Figs. 3 and 8), but rather varies between $2\pi/L_A$ and $2\pi/2L_A$, depending on the relative fractions of the two step heights.

#### b. *Steps of height $3d_{[111]}$ and $d_{[111]}$*

We find analogous results to those of Sec. III A for uncorrelated mixtures of steps of height $3d_{[111]}$ and $d_{[111]}$. Equal fractions of steps of these two heights produce very broad, unresolved peaks at the specular position at in-phase conditions for steps of height $3d_{[111]}$ (e.g., $S_\perp/S_{[111]}=3\frac{1}{3}$ and $3\frac{2}{3}$). Calculations for a small admixture of steps of height $d_{[111]}$ with steps predominantly of height $3d_{[111]}$ produce beam profiles similar to those of Sec. I A, i.e., for a regular staircase containing steps of height $3d_{[111]}$. For this case the calculated spacing in $S_\parallel$ between adjacent peaks is very close to $2\pi/3L_A$, but the peaks broaden away from the $n=3$ and 4 in-phase conditions, and the positions of the interference maxima depart slightly from straight lines in reciprocal space.


[1] R. Fischer, H. Morkoç, D. A. Neumann, H. Zabel, C. Choi, N. Otsuka, M. Longerbone, and L. P. Erickson, J. Appl. Phys. **60**, 1640 (1986).

[2] M. Tsuchiya, P. M. Petroff, and L. A. Coldren, Appl. Phys. Lett. **54**, 1690 (1989), and references therein.

[3] S. T. Chui and J. D. Weeks, Phys. Rev. B **23**, 2438 (1981).

[4] D. J. Chadi, Ultramicrosc. **31**, 1 (1989), and references therein.

[5] E. M. Pearson, T. Halicioglu, and W. A. Tiller, Surf. Sci. **184**, 410 (1987); D. E. Aspnes and J. Ihm, Phys. Rev. Lett. **57**, 3054 (1986).

[6] R. J. Phaneuf and E. D. Williams, Phys. Rev. Lett. **58**, 2563 (1987).

[7] R. J. Phaneuf, E. D. Williams, and N. C. Bartelt, Phys. Rev. B **38**, 1984 (1988).

[8] N. C. Bartelt, E. D. Williams, R. J. Phaneuf, Y. Yang, and S. Das Sarma, J. Vac. Sci. Technol. A **7**, 1898 (1989).

[9] For a recent review article on the topic of equilibrium crystal shape, see C. Rottman and M. Wortis, Phys. Rep. **103**, 59 (1984).

[10] B. Z. Olshanetsky and A. A. Shklyaev, Surf. Sci. **82**, 445 (1979).

[11] V. I. Mashanov and B. Z. Olshanetskii, Pis'ma Zh. Eksp. Teor. Fiz. **36**, 290 (1982) [JETP Lett. **36**, 356 (1982)].

[12] F. Jentzsch and M. Henzler, Appl. Phys. A **46**, 119 (1988).

[13] M. Henzler, Surf. Sci. **36**, 109 (1973).

[14] R. S. Becker, J. A. Golovchenko, E. G. MacRae, and B. S. Schwartzentruber, Phys. Rev. Lett. **55**, 2028 (1985).

[15] W. Telieps and E. Bauer, Surf. Sci. **162**, 163 (1985).

[16] W. P. Ellis and R. L. Schwoebel, Surf. Sci. **11**, 82 (1968).

[17] M. Henzler, in *Electron Spectroscopy for Surface Analysis,* edited by H. Ibach (Springer, Berlin, 1977).

[18] The assignment of the angular position corresponding to $S_\parallel=0$ is done by measuring the angular width of each component peak as a function of incident energy and noting the position of the peak at which this width has a minimum. There is some uncertainty in this procedure owing to the finite angular resolution of our diffractometer, as well as inhomogeneities in the LEED optics. We assign an uncertainty of $\pm2$ eV to the position in energy, or an uncertainty in $S_\perp$ of $\pm0.08$ times $(2\pi/d_{[111]})$, for the in-phase conditions shown.

[19] J. L. Souchiere and V. T. Binh, Surf. Sci. **168**, 52 (1986).

[20] E. Bauer, M. Mundschau, W. Święch, and W. Telieps, in Eval-

uation of Advanced Semiconductor Materials by Electron Microscopy, edited by D. Cherns (Plenum, New York, in press).

[21]N. Okasabe, Y. Tanishiro, K. Yagi, and G. Honjo, Surf. Sci. **97**, 393 (1980).

[22]M. G. Lagally, T. C. Ngoc, and M. B. Webb, Phys. Rev. Lett. **26**, 1557 (1971).

[23]Plotting the profiles as a function of $S_{\parallel}$ produces an apparent broadening of the peaks with increasing energy (and therefore $S_{\perp}$). In fact, the angular widths of the peaks in the profiles at energies of 35 and 63 eV are the same; the angular peakwidths in the middle of the energy range for which data are shown in both Figs. 3 and 8, i.e., near 49 eV, are somewhat larger.

[24]J. E. Houston and R. L. Park, Surf. Sci. **21**, 209 (1970).

[25]J. M. Pimbley and T.-M. Lu, J. Appl. Phys. **55**, 182 (1983).

[26]P. R. Pukite, C. S. Lent, and P. I. Cohen, Surf. Sci. **161**, 39 (1985).

[27]For the 6° misorientation, we measure the FWHM of a number of seventh-order beams to be $\Delta S_{\parallel}=0.10\pm0.02$ Å$^{-1}$ at an incident energy of 50 eV and an incident angle of 10° compared to an estimate of the instrument limit of 0.065 Å$^{-1}$ at these conditions. The fraction of the beam width one attributes to finite-size broadening depends on how one attempts to deconvolve the instrument response from the beam profile. We take as limits the cases where in the convolution the component widths simply add, and where they add in quadrature; this yields limits on the finite-size beam broadening of $0.035\pm0.007$ and $0.076\pm0.015$ Å$^{-1}$, respectively. Taking $2\pi$ over these values to be a measure of the average domain size yields upper and lower limits of $180\pm40$ and $80\pm20$ Å.

[28]We obtain an estimate of the reconstructive transition temperature on the singular Si(111) surface by an extrapolation of our transition temperatures versus misorientation angle on surfaces misoriented toward $[1\bar{1}0]$ to 0° misorientation (cf. Ref. 7). This yields a transition temperature of $865\pm5$ °C on the singular surface.

[29]K. Takayanagi, K. Tanashiro, M. Takahashi, and S. Takahashi, J. Vac. Sci. Technol. A **3**, 1502 (1985).

[30]W. Telieps and E. Bauer, Ber. Bunsenges. Phys. Chem. **90**, 197 (1986).

[31]R. L. Schwoebel and E. J. Shipsey, J. Appl. Phys. **37**, 3682 (1966).

[32]For an early discussion of whether the configuration of steps at high temperature is determined by equilibrium or kinetic considerations, see A. J. W. Moore, in *Metal Surfaces,* edited by W. D. Robertson and N. A. Gjostein (Am. Soc. for Metals, Metals Park, Ohio, 1963), p. 155.

[33]N. Okasabe, Y. Tanishiro, K. Yagi, and G. Honjo, Surf. Sci. **109**, 353 (1981).

[34]Y.-W. Mo, B. S. Schwartzentruber, M. B. Webb, and M. G. Lagally, Bull. Am. Phys. Soc. **34**, 466 (1989).

[35]M. B. Webb and M. G. Lagally, in Vol. 28 of *Solid State Physics,* edited by H. Ehrenreich, F. Seitz, and D. Turnbull (Academic, New York, 1973), p. 301.

[36]For our instrument, measurements of beam profiles from carefully annealed surfaces at in-phase conditions indicates a response function which is approximately Gaussian in its center, with an angular full width at half maximum of approximately 0.9°, nearly independent of incident energy over the range for which we present data.

[37]H. Huang, S. Y. Tong, W. E. Packard, and M. B. Webb, Phys. Lett. **130A**, 166 (1988).

[38]For this calculation for the 12° misorientation the scatterers are arranged in (111) terraces 7 spacings wide alternating with pairs of (111) terraces, each 2 spacings wide.

[39]A broadening of the peaks due to the finite size of the patches has been neglected in Fig. 13. This does not change the peak positions or relative intensities.

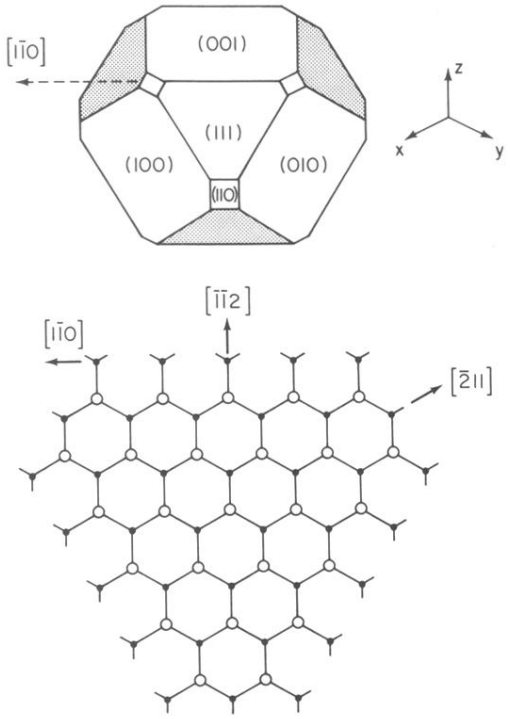


FIG. 1. Schematic of Si(111) surface in relation to other low index surfaces. The schematic of the bulk-terminated (111) surface in the lower panel is shown in the same orientation as the (111) face in the upper panel. Misorientation directions of the vicinal surfaces studied in this and previous work are indicated by arrows.

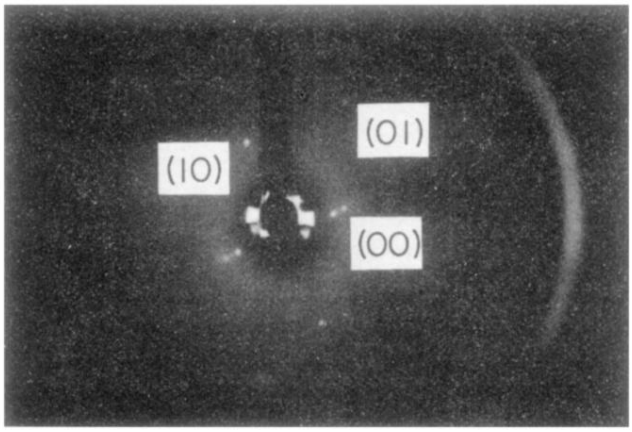


FIG. 2. LEED pattern for a vicinal Si(111) surface misoriented 6° toward $[2\bar{1}\,\bar{1}]$ at 870°C. Incident energy = 48 eV. Incident angle = 10° with respect to [111]. Specular and first-order (111) reflections are indicated. First-order reciprocal-lattice vector is of magnitude $|a^*| = 1.889$ Å$^{-1}$

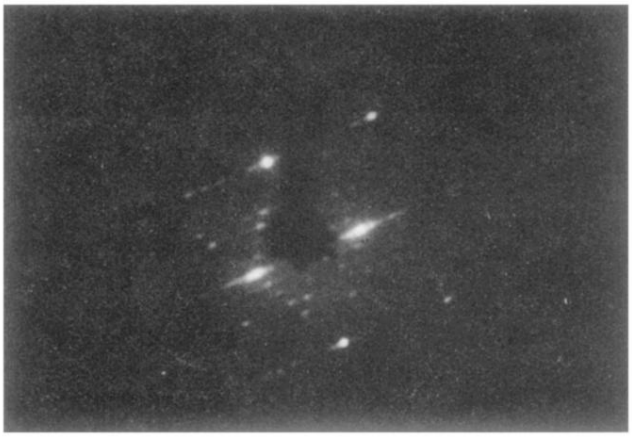

FIG. 4. LEED pattern for a vicinal Si(111) surface misoriented by 6° toward $[2\bar{1}\,\bar{1}]$ at 360 °C. Incident energy = 48 eV. Incident angle = 10° with respect to [111]. Reflection positions and scale as in Fig. 2.